No. PO8C05 Transactions of the Korean Nuclear Society Autumn Meeting Changwon, Korea, October 24-25, 2024

Application of iterative reconstruction algorithms to limited-angle tomography

Seokwon Oh, Seungjun Yoo, Junho Lee, Seongbon Park, Taehoon Kim, and Ho Kyung Kim*

Radiation Imaging Laboratory, School of Mechanical Engineering, Pusan National University, 2, Busandaehak-ro 63beon-gil, Geumjeong-gu, Busan 46241, Republic of Korea

*Correspondence: hokyung@pusan.ac.kr

Speaker: seokwonoh@pusan.ac.kr

Motivation

- Limited-angle tomography (LAT) is a solution for inspecting the objects when the full 360° scanning is not feasible
- However, the incomplete data acquired from less than 180° scans introduces out-of-plane and streak artifacts in the reconstructed images, which are intensified in conventional methods such as the filtered backprojection (FBP)
- Iterative reconstruction (IR) methods can be an alternative to reduce out-of-plane artifacts compared to FBP, but they may still be insufficient, leading this study to investigate IR algorithms with prior images

Objectives

- To apply various IR methods to LAT, given as the system of linear equations (with and without regularization) and statistical maximum likelihood
- To compare the performance of IR methods using ideal detectability, artifact-spread function (ASF), and structural similarity index measure (SSIM)
- To compare the reconstruction results of IR and prior-image constrained IR for simulation data

Materials and Methods

Simulation phantom

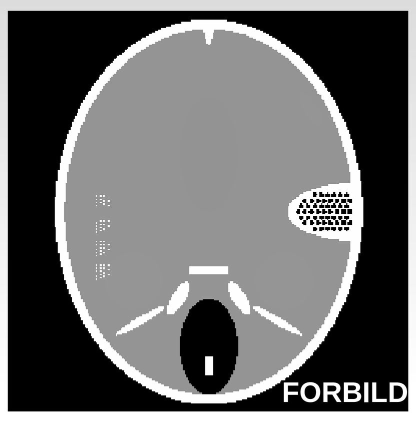

Experimental setup

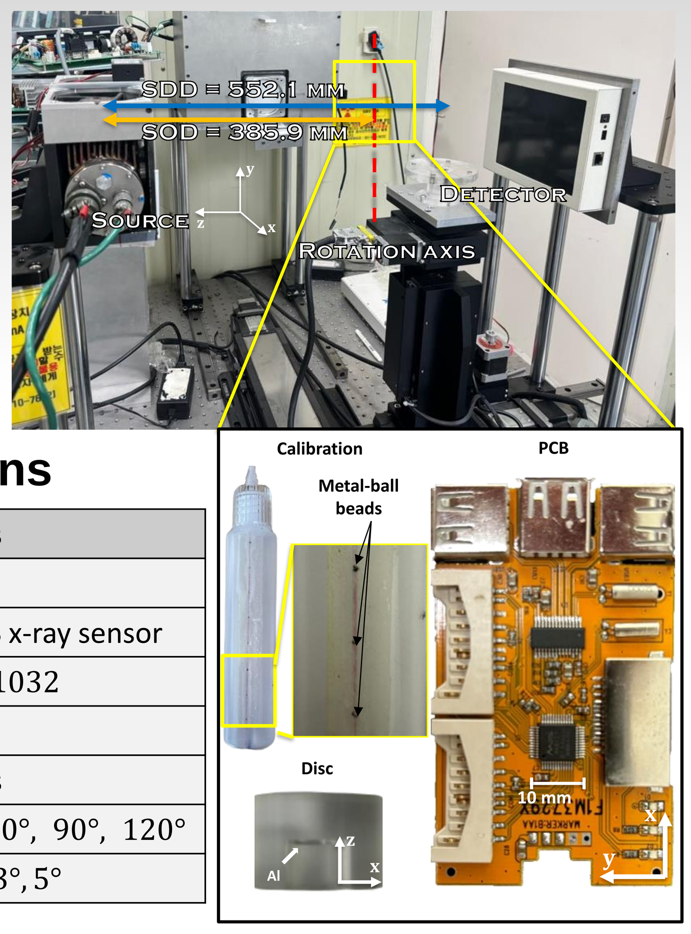

CT system specifications

Category	Details
X-ray	45 kVp, 0.1593 mGy/s
Detector	Shad-o-Box HS, CMOS x-ray sensor
	Pixel format: 1548 × 1032
	Pixel pitch: 99 μm
	Readout time: 200 ms
Scan	Scan range (α): 30°, 60°, 90°, 120°
	Step angle(β): 1°, 2°, 3°, 5°

Algorithms used for reconstruction

- **Feldkamp, Davis, Kress (FDK), Hann filter**
  $x = \int \frac{1}{\Lambda^2} \int_{-\infty}^{\infty} \frac{L_{SD}}{\sqrt{L_{SD}^2+\xi^2+\zeta^2}} b_\theta(\xi,\zeta) * h(\xi'-\xi)\, \mathrm{d}\zeta \mathrm{d}\theta$
- **Simultaneous algebraic reconstruction technique (SART)**
  $\mathbf{x}^{k+1} = \mathbf{x}^k + \lambda^k \frac{A^T(\mathbf{b}-\mathbf{A}\mathbf{x}^k)}{\mathbf{A}^T\mathbf{A}\mathbf{1}}$
- **Conjugate gradient least squares (CGLS)**
  $\mathbf{r}_0 = \mathbf{b} - \mathbf{A}\mathbf{x}^0,\ \mathbf{p}_0 = \mathbf{A}^T\mathbf{r}_0$
  $\mathbf{x}^{k+1} = \mathbf{x}^k + \frac{\|\mathbf{p}_k\|_2^2}{\|\mathbf{A}\mathbf{x}^k\|_2^2}\mathbf{p}_k$
  $\mathbf{r}_{k+1} = \mathbf{r}_k - \frac{\|\mathbf{p}_k\|_2^2}{\|\mathbf{A}\mathbf{x}^k\|_2^2}\mathbf{A}\mathbf{p}_k$
  $\mathbf{p}_{k+1} = \mathbf{A}^T\mathbf{r}_{k+1} + \frac{\|\mathbf{A}^T\mathbf{r}_{k+1}\|_2^2}{\|\mathbf{A}^T\mathbf{r}_k\|_2^2}\mathbf{p}_k$
- **Maximum likelihood-expectation maximization (MLEM)**
  $\mathbf{x}^{k+1} = \mathbf{x}^k \cdot \frac{\mathbf{A}^T\left(\frac{\mathbf{b}}{\mathbf{A}\mathbf{x}^k}\right)}{\mathbf{A}^T\mathbf{1}}$
- **SART with total variation regularization (SART-TV)**
  $\mathbf{x}^* = \arg\min_{\mathbf{x}} \|\mathbf{x}\|_{TV}$, subject to $\mathbf{A}\mathbf{x} = \mathbf{b}$
- **Prior image constrained compressed sensing (PICCS)**
  $\mathbf{x}^* = \arg\min_{\mathbf{x}} \left((\mathbf{1}-\boldsymbol{\alpha})\|\mathbf{x}-\mathbf{x}_p\|_{\mathbf{TV}} + \boldsymbol{\alpha}\|\mathbf{x}\|_{\mathbf{TV}})\right)$
- **Stopping criteria**
  when $\|\mathbf{A}\mathbf{x}^{k+1}-\mathbf{b}\|_2 > \|\mathbf{A}\mathbf{x}^k-\mathbf{b}\|_2$

Evaluation method

- Contrast-to-noise ratio (CNR)
  - Calculate the CNR of a 0.5 mm thick Al disc phantom
  - Normalize the squared CNR by the number of projection views used for reconstruction, which is equivalent to the ideal detectability
  - $\mathrm{CNR} = \frac{\bar{\mu}_{\mathrm{ROI}}(0)-\bar{\mu}_{\mathrm{Bg}}(0)}{\sigma}$, where $\sigma = \sqrt{\frac{\sigma_{\mathrm{ROI}}^2+\sigma_{\mathrm{Bg}}^2}{2}}$
- Relative contrast
  - Calculate the relative contrast in an in-pane (x-y) image of the Al disc phantom
  - $2\frac{\bar{\mu}_{\mathrm{ROI}}-\bar{\mu}_{\mathrm{Bg}}}{\bar{\mu}_{\mathrm{ROI}}+\bar{\mu}_{\mathrm{Bg}}}$
- Relative noise
  - Calculate the relative noise in an in-pane (x-y) image of the Al disc phantom
  - $\sqrt{2}\frac{\sqrt{\sigma_{\mathrm{ROI}}^2+\sigma_{\mathrm{Bg}}^2}}{\bar{\mu}_{\mathrm{ROI}}+\bar{\mu}_{\mathrm{Bg}}}$
- Artifact-spread function (ASF)
  - Estimate the streak artifact from the ASF obtained for an Al disc phantom
  - $\mathrm{ASF}(z) = \frac{\bar{\mu}_{\mathrm{ROI}}(z)-\bar{\mu}_{\mathrm{Bg}}(z)}{\bar{\mu}_{\mathrm{ROI}}(0)-\bar{\mu}_{\mathrm{Bg}}(0)}$
- Structural similarity index measure (SSIM)
  - $\mathrm{SSIM}(x,y) = \frac{(2\mu_x\mu_y+c_1)(\sigma_{xy}+c_2)}{(\mu_x^2+\mu_y^2+c_1)(\sigma_x^2+\sigma_y^2+c_2)}$
    μ: the pixel sample mean of x and y (kernel)
    σ: the variance of x and y
    σ_{xy}: the covariance of x and y

- **Disc phantom**

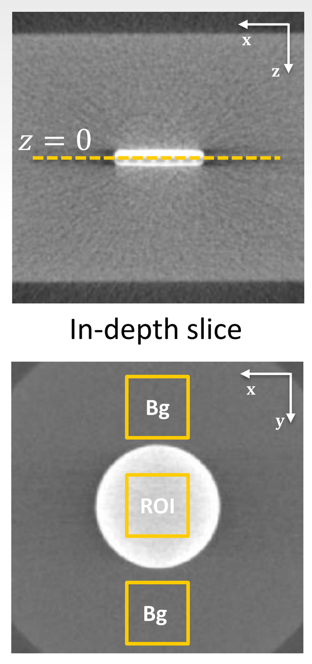

Results

Ideal detectability

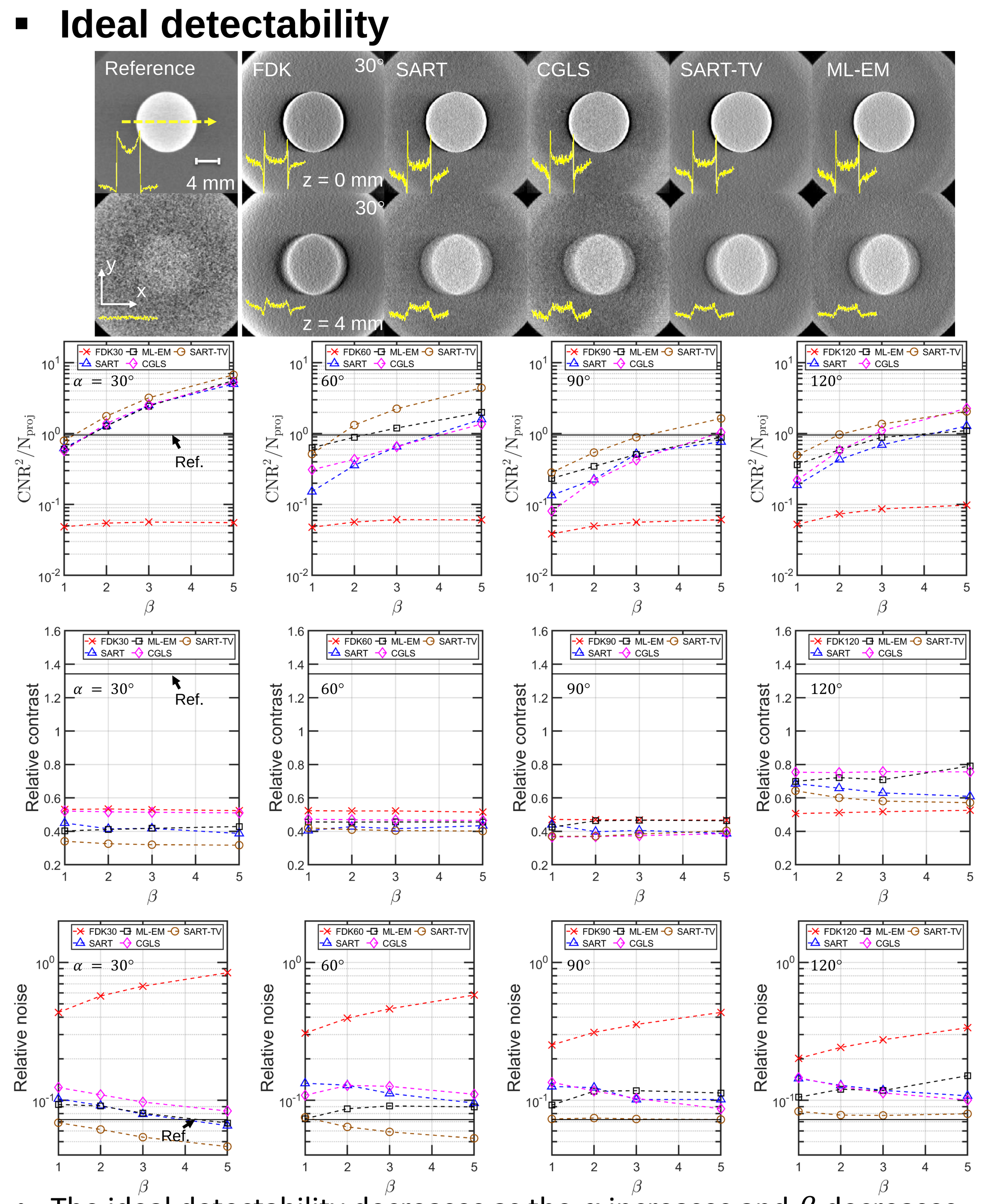

- The ideal detectability decreases as the α increases and β decreases
- IR methods demonstrate higher ideal detectability than FDK
- In terms of relative contrast, there is no significant difference between algorithms except for $\alpha = 120°$
- The IR methods show better noise performance than FDK, with SART-TV being the best

Artifact-spread function

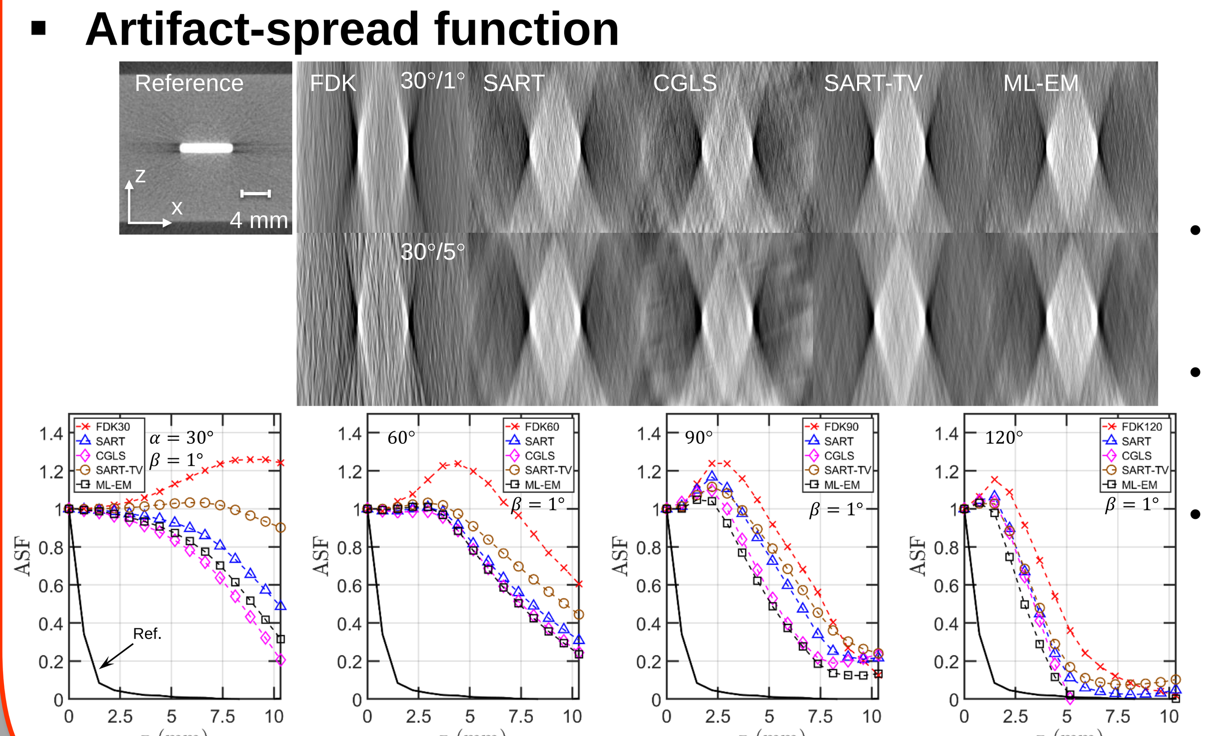

- The artifact-spreading decreases as the α increases
- The IR methods show lower artifact-spreading than FDK
- However, the difference is marginal as the α increases

PCB reconstruction result

- **In-plane images ($\alpha = 60°, \beta = 1°$)**

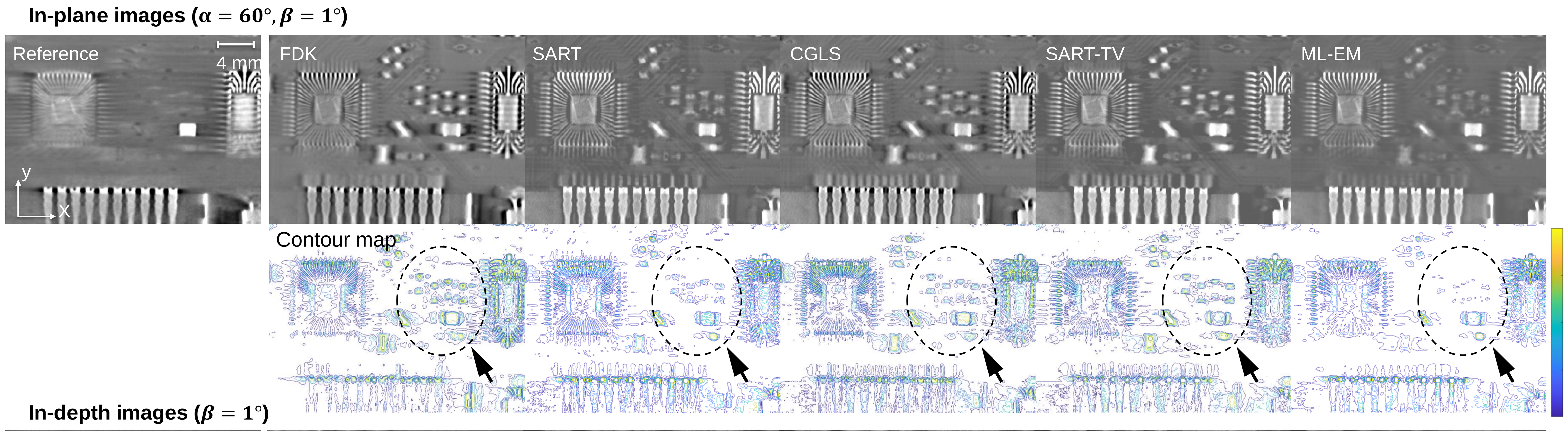

- **In-depth images ($\beta = 1°$)**

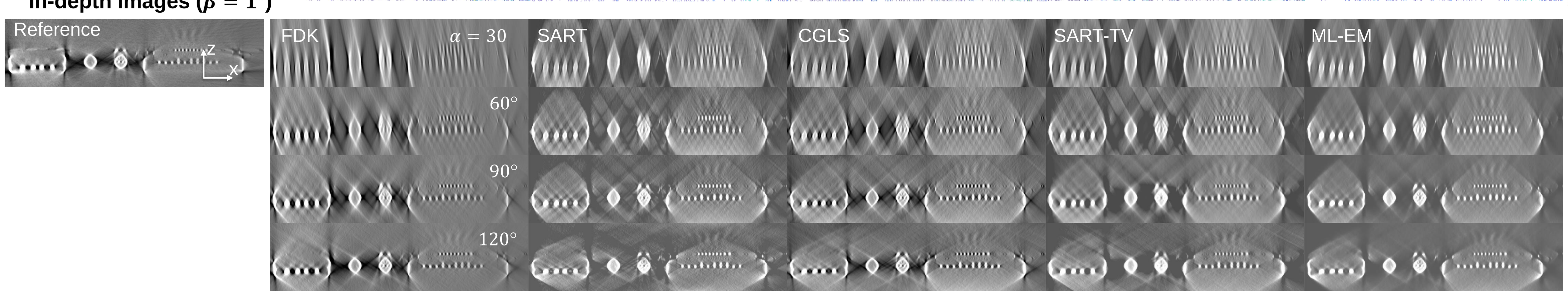

- IR methods shows less out-of-plane artifacts, and among IR methods the ML-EM is the best; however, the difference is marginal
- The out-of-plane artifacts can be well seen in in-depth view, and the artifacts decrease as the α increases

FORBILD reconstruction result

- $\alpha = 120°,\ \beta = 5°$
- $\alpha = 120°,\ \beta = 10°$

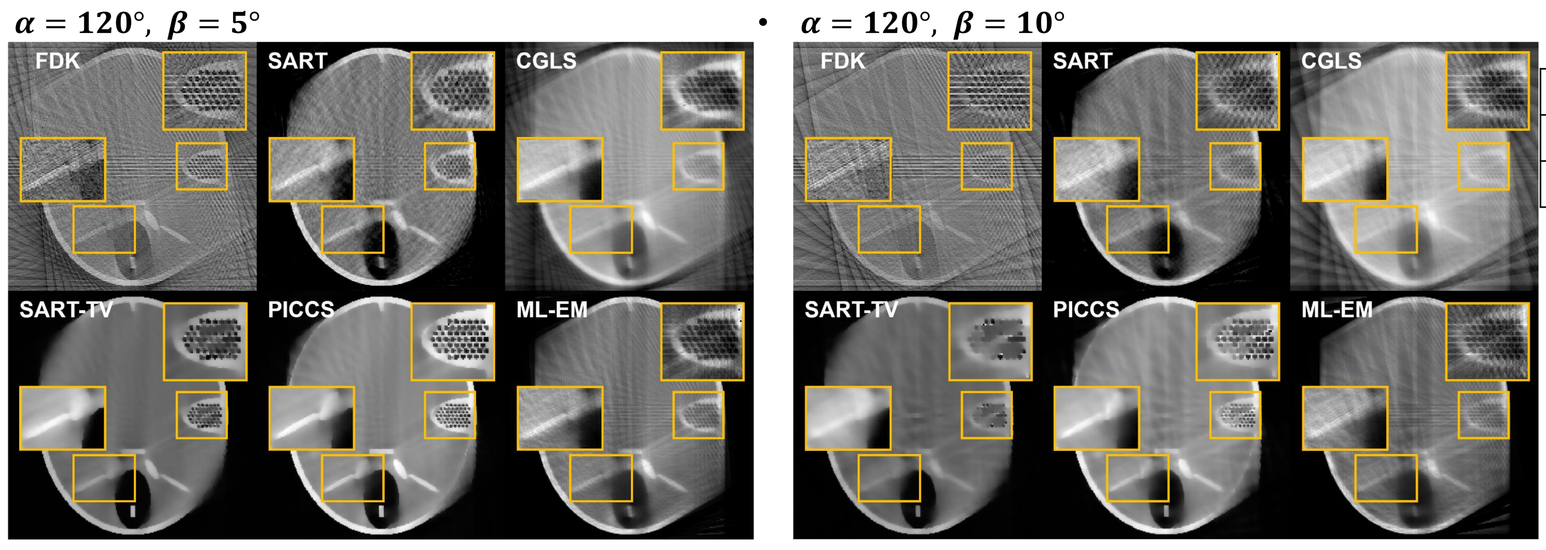

$\beta = 5°/10°$	FDK	SART	CGLS	SART-TV	PICCS	ML-EM
SSIM	0.077 / 0.052	0.471 / 0.469	0.252 / 0.209	0.747 / 0.631	**0.762 / 0.664**	0.524 / 0.504
MSE	0.693 / 1.477	0.038 / 0.047	0.092 / 0.103	0.029 / 0.041	**0.028 / 0.038**	0.055 / 0.060

- The IR methods are superior to the FDK but still suffer from the streak artifacts
- The prior image used algorithm (PICCCS) shows the well-preserving detail of the phantom and shows the best performance among all methods

Discussion

- The ideal detectability increases as the α increases, which is one of the advantages of LAT
- Unlike our expectation that all IR algorithms would outperform the FDK in every aspect, the streak artifacts in particular, the overall performance of SART, CGLS, and SART-TV are comparable to that of FDK in experiments
- However, in terms of noise, IR methods generally offer superior performance
- PICCS, which utilizes the prior image, reduces artifacts and demonstrates a significant advantage in preserving structural details

Radiation Imaging Laboratory {http://ril.pusan.ac.kr}

This work was supported by the National Research Foundation of Korea (NRF) grant funded by the Korea government (MSIT) (No. 2021R1A2C1010161). S. Oh was supported by Basic Science Research Program through the NRF funded by the Ministry of Education (No. RS-2024-00408137)